Princeton Plasma Physics Laboratory

PPPL-5383

Destabilization of counter-propagating Alfvénic instabilities by off-axis, co-current neutral beam injection

M. Podestà, E. D. Fredrickson and M. Gorelenkova

April 2017

Prepared for the U.S. Department of Energy under Contract DE-AC02-09CH11466.

Princeton Plasma Physics Laboratory
Report Disclaimers

Full Legal Disclaimer

This report was prepared as an account of work sponsored by an agency of the United States Government. Neither the United States Government nor any agency thereof, nor any of their employees, nor any of their contractors, subcontractors or their employees, makes any warranty, express or implied, or assumes any legal liability or responsibility for the accuracy, completeness, or any third party's use or the results of such use of any information, apparatus, product, or process disclosed, or represents that its use would not infringe privately owned rights. Reference herein to any specific commercial product, process, or service by trade name, trademark, manufacturer, or otherwise, does not necessarily constitute or imply its endorsement, recommendation, or favoring by the United States Government or any agency thereof or its contractors or subcontractors. The views and opinions of authors expressed herein do not necessarily state or reflect those of the United States Government or any agency thereof.

Trademark Disclaimer

Reference herein to any specific commercial product, process, or service by trade name, trademark, manufacturer, or otherwise, does not necessarily constitute or imply its endorsement, recommendation, or favoring by the United States Government or any agency thereof or its contractors or subcontractors.

PPPL Report Availability

Princeton Plasma Physics Laboratory:

http://www.pppl.gov/techreports.cfm

Office of Scientific and Technical Information (OSTI):

http://www.osti.gov/scitech/

Related Links:

U.S. Department of Energy

U.S. Department of Energy Office of Science

U.S. Department of Energy Office of Fusion Energy Sciences

Destabilization of counter-propagating Alfvénic instabilities by off-axis, co-current neutral beam injection

M. Podestà, E. D. Fredrickson and M. Gorelenkova
Princeton Plasma Physics Laboratory, NJ 08543 - US
(Dated: April 19, 2017)

Injection of high-energy neutrals (NBI) is a common tool to heat the plasma and drive current non-inductively in fusion devices. Once neutrals ionize, the resulting energetic particles (EP) can drive instabilities that are detrimental for the performance and the predictability of plasma discharges. A broad NBI deposition profile, e.g. by off-axis injection, is often assumed to limit those undesired effects by reducing the radial gradient of the EP density, thus reducing the drive for instabilities. However, this work presents new evidence that off-axis NBI can also lead to undesired effects such as the *destabilization* of Alfvénic instabilities. Time-dependent analysis with the TRANSP code indicates that instabilities are driven by a combination of radial and energy gradients of the EP distribution. The mechanisms for wave-particle interaction revealed by the EP phase space resolved analysis are the basis to identify strategies to mitigate or suppress the observed instabilities.

The reliable operation of fusion reactors such as ITER requires accurate predictions of scenarios that feature large populations of energetic particles (EP) from fusion reactions, neutral beam injection (NBI) and rf waves. Although NBI is a well-proven tool for heating and current drive, the resulting EP population can drive instabilities such as Alfvénic modes (AEs) [1][2][3][4][5]. Destabilization of AEs typically causes a degradation in performance. If significant EP losses are induced, damage of vacuum vessel components can also occur.

Scenarios with a broad EP pressure profile from off-axis NBI are usually thought to be effective in limiting EP-driven modes, under the main assumption that the drive from the radial EP density gradient is the main energy source for the instabilities. Examples from recent experiments are reported, for example, in Ref. [6]. In contrast, this work reports the first experimental evidence of the *destabilization* of toroidicity-induced AEs (TAEs) by off-axis, co-current NBI. Notably, the observed TAEs propagate in the *counter*-current direction in spite of the co-NB injection. Experimental observations are qualitatively explained by inversions in the radial gradient of the EP density. However, in general, the intrinsic coupling between EP redistribution in energy and radius (caused by wave-particle interactions) must be considered for a more quantitative understanding of the experimental results. For example, the formation of EP distributions with inverted fast ion energy gradients caused by simultaneous NB and rf injection in reactors such as ITER can further reduce the stability of counter-propagating TAEs [7][8]. Therefore, reliable predictions for future scenarios on ITER and other reactor-grade devices should be based on analyses that include the entire EP phase space dynamics, especially when a complex EP distribution function is expected from the synergy between fusion reactions, NBI and rf heating.

Experimental scenario. This work is based on experimental observations from the National Spherical Torus Experiment Upgrade (NSTX-U [9]), which is equipped with up to 12 MW of neutral beam power for non-inductive heating and current drive. NSTX-U is a small aspect ratio device (major/minor radius are 0.95 m and 0.65 m respectively) operating at nominal magnetic field $B_T \leq 1$ T and plasma current ≤ 2 MA. The experiments discussed herein are low-confinement mode, deuterium plasmas. Density and temperature are $n_e \approx 2.5 \times 10^{19}$ m^{-3} and $T_e \approx T_i \leq 1$ keV (subscripts e, i refer to electrons and ions, respectively). Plasma current increases during the time of interest, $100 \leq t \leq 400$ ms, and reaches 0.9 MA during flat-top (Fig. 1) at $B_T = 0.65$ T. A common feature for NSTX-U discharges exhibiting counter-propagating TAEs is NB injection of 0.9 MW in the co-current direction from a NB source with tangency radius $R_{tan} = 130$ cm, that is near mid-radius on the outboard midplane.

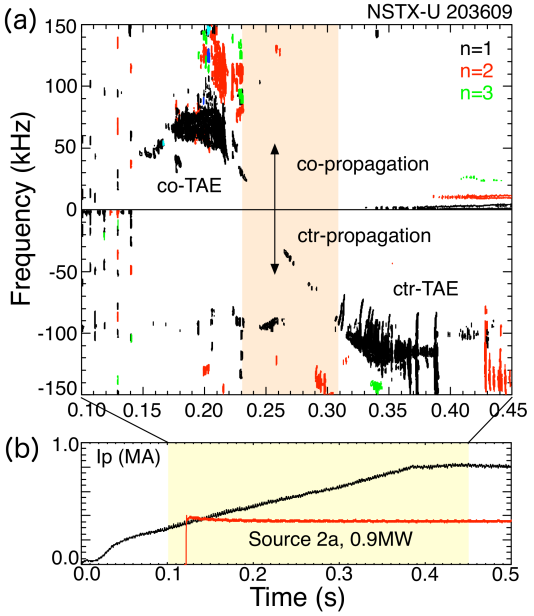

FIG. 1: (a) Spectrum of magnetic fluctuations measured by Mirnov coils. Counter-propagating modes are here shown with negative frequency. (b) Waveforms of plasma current (black) and injected NB power (red).

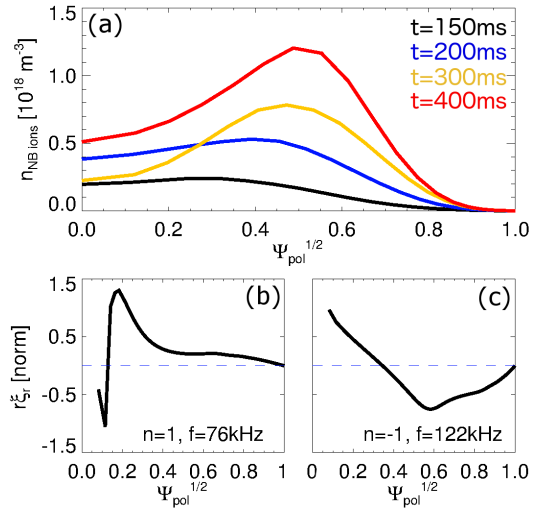

FIG. 2: (a) NB ion density profile vs time. (b-c) Radial displacement, $r\xi_r$, for co- and counter-propagating $|n| = 1$ TAE eigenmodes from NOVA analysis. (r: normalized minor radius).

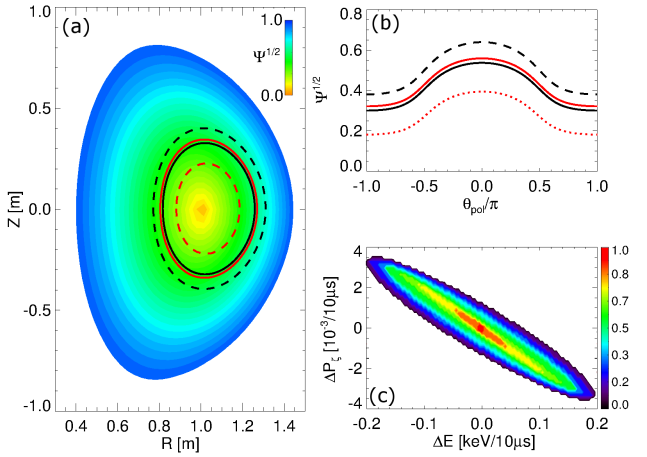

FIG. 3: (a) Poloidal cross-section with contours at constant poloidal flux, $\Psi^{1/2}$. Lines show orbits for $E = 20$ keV particles (solid) that gain (black, dashed) or lose (red, dashed) energy through interaction with a counter-TAE. (b) Particle position vs poloidal angle. Note the large departure from the initial flux surface ($\theta_{pol} = 0$) during the orbiting. (c) Kick probability associated with the particle's (E, P_ζ, μ) for a counter-TAE.

An example of these discharges is shown in Fig. 1. Soon after NB injection starts, toroidal Alfvén eigenmodes (TAEs) are driven unstable by the increasing population of fast particles. Figure 1 shows the spectrum of magnetic fluctuations measured at the plasma edge by Mirnov coils, from which toroidal mode numbers $|n| = 1, 2$ are computed. The direction of propagation of the TAEs can be inferred from the relative phase of detectors distributed toroidally around the vacuum vessel. Early in time, TAEs propagate in the co-NB injection direction. However, at later times a reversal in the direction of propagation is observed and TAEs propagate in the *counter*-NB injection direction after 300 ms.

TRANSP analysis of TAE destabilization. The destabilization of counter-TAEs is investigated through the time-dependent tokamak transport code TRANSP [10][11], whose NB module NUBEAM [12][13] has been recently enhanced with a physics-based, reduced model for fast ion transport by instabilities (called *kick model* [14]). The kick model in NUBEAM/TRANSP is here used to compute mode stability (linear growth rate γ_{lin}), hence the net growth rate γ_{net} that includes damping rates from NOVA [15]. Thermal plasma profiles are used as input for the NOVA code to compute the eigenmodes for $|n| = 1$ TAEs. Since the background profiles and the fast ion distribution are rapidly evolving during the current ramp (Fig. 2a), the NOVA analysis is performed at two representative times, 200 ms and 320 ms, corresponding to the peak activity of TAEs. Eigenmodes from NOVA are used in the particle following code ORBIT [16] to compute the phase-space resolved transport probability matrix associated with each mode [14]. Probability matrices are then used in TRANSP/NUBEAM to investigate the mode's stability [15]. In the following, fast ion coordinates in phase space are identified by the constants of motion E, P_ζ and μ [17]. E is the total particle energy. $P_\zeta = \rho_\parallel g/\Psi_w - \Psi_{pol}$ is the canonical angular momentum ($\rho_\parallel$: parallel particle momentum; $g \sim B/R$: the g-function; Ψ_{pol}: poloidal flux; Ψ_w: value of Ψ_{pol} at the wall). μ is the magnetic moment.

Figure 3 illustrates the advantage of adopting phase space over real space representation to investigate mode stability. Orbits are shown for two particles with same initial energy $E = 20$ keV and position at the mid-plane $\Psi_{pol} \approx 0.4$. After interacting for 4 ms with a counter-TAE, one particle gains energy and the other loses energy, with $|\Delta E| = 4$ keV. Away from the mid-plane, particles depart from the initial position and explore a large radial range of Ψ_{pol} (Fig. 3b). The same orbits appear as simpler trajectories in terms of (E, P_ζ, μ), with the effect of the mode represented by the kick probability shown in Fig. 3c.

The correlation between energy and P_ζ changes visible in Fig. 3c is expected from the fundamental relationship induced by resonant wave-particle interactions, with $\Delta P_\zeta/\Delta E \sim n/\omega$ [17]. The computation of the correlated ΔE and ΔP_ζ kicks over the phase space (E, P_ζ, μ) is at the basis of the kick model. ΔE and ΔP_ζ kicks can be visualized over the entire phase space through their root-mean-square value as a function of (E, P_ζ, μ) (Fig. 4). One notable feature are the large variations of the probabilities over the (E, P_ζ, μ) space. This results from the localization of resonances in phase space and from the (generally) large number of resonances associated with each mode.

Linear stability. Kick probabilities are computed for all candidate eigenmodes from NOVA, then used in TRANSP to infer the mode stability (Fig. 5). Only two

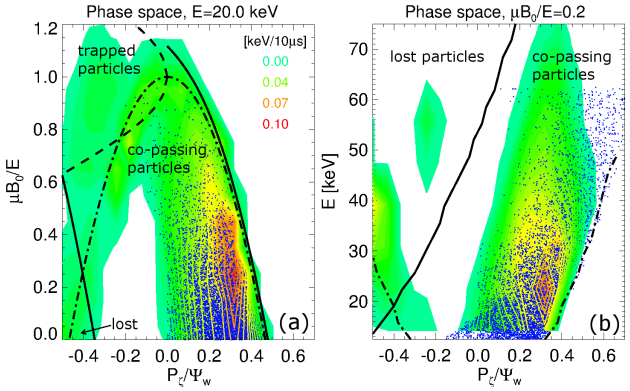

FIG. 4: Contours show the phase space map of the root-mean-square energy kicks from the counter-TAE in Fig. 2c. Lines represent boundaries between different types of orbit. Dots are a sample of the fast ion distribution from NUBEAM/TRANSP.

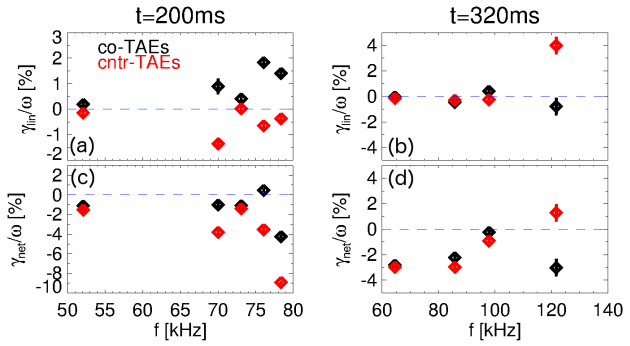

FIG. 5: Linear stability through TRANSP and kick model for co-TAEs (black) and counter-TAEs (red). (a-b) Linear growth rate. (c-d) Net linear growth rate, including damping rate from NOVA-K.

of the original eigenmodes from NOVA are found to be unstable, namely a co-TAE with frequency $f \approx 76$ kHz at $t = 200$ ms and a counter-TAE with $f \approx 122$ kHz at $t = 320$ ms. Their radial mode structure is shown in Figs. 2b-c. Only these two modes are retained in the following analysis.

More details of the stability results for the two unstable modes are presented in Fig. 6. For the co-propagating TAE, the linear growth rate exceeds the damping rate after 150 ms, it increases rapidly up to ≈ 180 ms and then decreases until the mode is stabilized. The counter-propagating mode shows the opposite behavior. The linear growth rate is *negative* at earlier times, then increases and the mode is destabilized after ≈ 250 ms. Because of the fast variation in background plasma profiles, however, the validity of the computed transport probability is questionable outside time windows of $\pm 30-50$ ms from the selected times $t = 200$ ms and $t = 320$ ms. Nevertheless, the trends shown in Figs. 6a appear quite robust and overall consistent with the experimental behavior of the modes, cf. Fig. 1a.

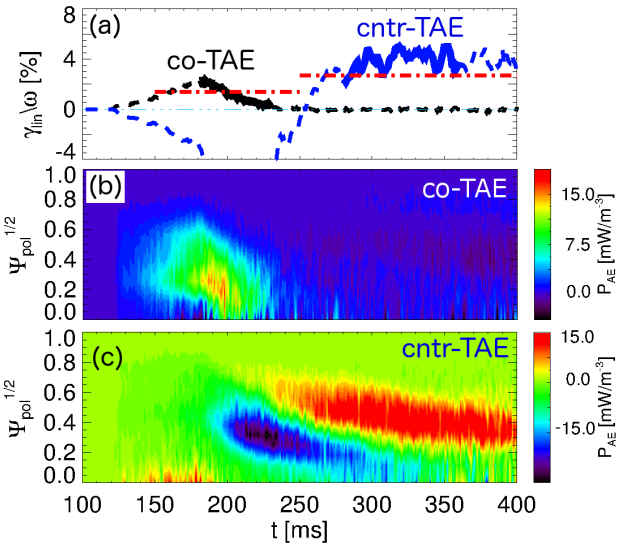

FIG. 6: (a) Linear growth rate of the most unstable $n = 1$ TAEs vs time. Dashed line indicates the time range over which kick model results become unreliable. Red dot-dashed line is the damping rate from NOVA-K. (b-c) Radial profile of the power exchanged between fast ions and the mode in the linear phase. Positive power means energy is transferred from the particles to the wave.

Figures 6b-c show the radial profiles of power transferred from fast ions to each mode in the limit of vanishing mode amplitude (*linear* phase). It can be seen that most of the power is exchanged around $\Psi_{pol} = 0.2 - 0.5$, that is in the region of inverted radial gradient for $t \geq 200$ ms (Fig. 2a). Note that regions with both positive (destabilizing) and negative (stabilizing) energy transfer from the fast ions to the mode are observed, in spite of the monotonic density gradient. This reflects the competition between drive and damping by fast ions associated with the location of resonances in phase space, rather than in real space only.

Mode saturation. As unstable modes grow to a finite amplitude, fast ions respond to the instabilities and the *linear* response (cf. Fig. 6) is modified accordingly. Saturation amplitude can be estimated through the kick model by computing the mode amplitude for which power transferred from fast ions to the modes equals the power dissipated through damping [15].

The inferred saturation amplitudes are $\delta B/B \sim 5 - 10 \times 10^{-4}$ (δB: perturbation of the magnetic field) (Fig. 7) which is consistent with previous measurements on NSTX through reflectometry [15]. By comparing linear and saturated regimes, it is clear that the wave-particle interaction modifies the fast ion distribution, as seen for example from the modification of the power density profiles in panels (b,c) of Figs. 6-7. Changes in the profile when the square of mode amplitude (proportional to the wave energy) is scaled are shown in Fig. 8 for two representative times. The response of the fast ions causes a significant departure at saturation with respect to the

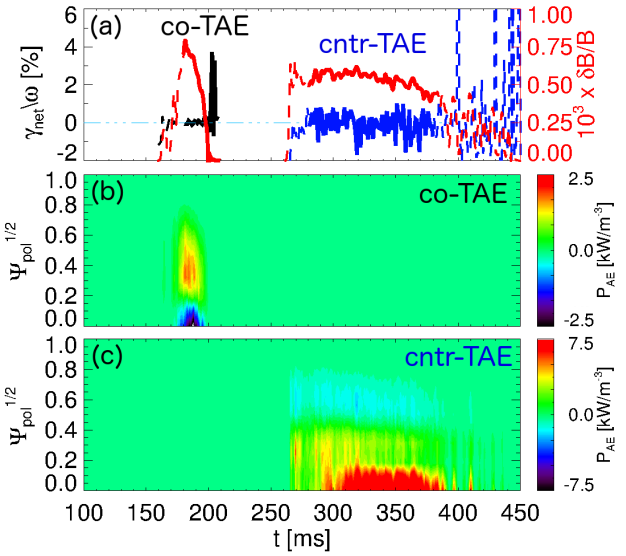

FIG. 7: (a) Black, blue: net growth rate near saturation. Red: saturation amplitude of most unstable $|n| = 1$ TAEs. Dashed lines indicate the time range over which kick model results are unreliable. (b-c) Radial profile of the power exchanged between fast ions and the mode in the saturated phase.

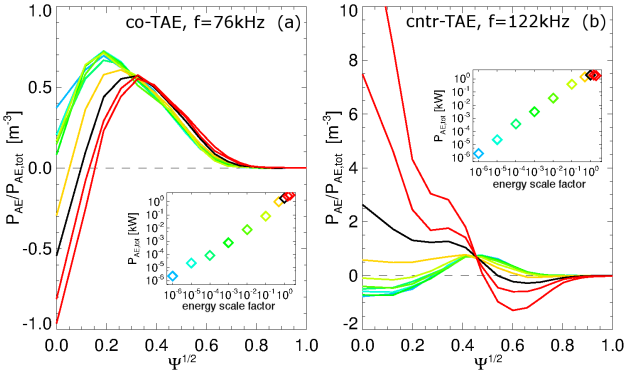

FIG. 8: Radial profile of power exchange between fast ions and co/counter-TAEs as the wave energy is increased. The insets show the total power vs wave energy scaling factor, where a factor 1 corresponds to the nominal saturation amplitude. All profiles are evaluated at $t = 200, 320$ ms for the co- and counter-TAE, respectively.

linear phase. For instance, the counter-TAE shows a reversal of the power density profile as the amplitude increases. Notably, from Fig. 8 the total power exchanged near and above saturation remains nearly constant, but the power density profile keeps evolving.

Discussion and conclusions. The competition between drive and damping by fast ions revealed by the stability analysis, along with the correlation $\Delta P_\zeta/\Delta E \sim n/\omega$, has three important implications. First, a simple linear stability analysis may not be representative of the mode's behavior near saturation (which where modes eventually become relevant in real experiments). Second, analysis based on the effect of a radial gradient alone may lead to incomplete or erroneous predictions for the mode's behavior. Third, a realistic EP distribution function, including sources/sinks and redistribution by the instabilities, must be used in the computation.

Counter-propagating TAE instabilities are observed on the NSTX-U device during off-axis, co-current NB injection. With density of energetic particles from off-axis NBI peaking around mid-radius, the hollow profile near the magnetic axis favors the destabilization of counter-TAEs [7]. However, detailed analysis with a realistic EP distribution shows that the positive EP density gradient near the axis is not enough to explain the positive growth rate of counter TAEs. For instance, no counter TAEs were observed in off-axis NBI experiments on the DIII-D device, in spite of the indications of hollow fast ion profiles [6]. One important difference between the scenarios in Ref. [6] and the work presented herein is that fast ions on NSTX-U are super-Alfvénic and therefore can access a broader set of resonances than on DIII-D.

The modes observed in NSTX-U have a broad radial structure that spans most of the minor radius, whereas much narrower structures are expected in devices such as ITER [4][18]. Nevertheless, regions with large mode activity can still be accessible to EPs whose orbit width is a considerable fraction of the minor radius, especially during the initial ITER operation at reduced plasma current and magnetic field. All these elements indicate that quantitative predictions of TAE stability and saturation should be performed in terms of phase space variables (E, P_ζ, μ) rather than simply assuming a predominant role of the universal TAE drive associated with the radial EP density gradient.

TRANSP analysis, augmented by a recent phase space resolved reduced EP transport model, can recover the experimental observations from NSTX-U. Results indicate the complex interplay between E and P_ζ gradients in driving TAEs unstable. The phase space resolved analysis provides the basic indications to mitigate or suppress the observed instabilities, e.g. by populating stabilizing regions of phase space by tailored NBI. Demonstration of such phase space engineering techniques will be pursued in future works.

Overall, the results presented in this work point to the need of phase space resolved analysis for quantitative predictions of TAE stability in future scenarios (e.g. in ITER), especially when a complex EP distribution function can originate from the synergy between NBI, rf injection and alpha particles from fusion reactions.

Acknowledgments

The contribution of the NSTX-U Team is gratefully acknowledged, as well as the invaluable advice of Drs. N. Gorelenkov, R. White and G. Kramer (PPPL) in using the NOVA/NOVA-K and ORBIT codes. This work is supported by the U.S. Department of Energy, Office

of Science, Office of Fusion Energy Sciences under contract number DE-AC02-09CH11466. NSTX-U at PPPL is a DOE Office of Science User Facility. The digital data for this paper can be found following the links from http://arks.princeton.edu/ark:/88435/dsp018p58pg29j.

[1] A. Fasoli, C. Gormezano, H. L. Berk, B. N. Breizman, S. Briguglio, D. S. Darrow, N. N. Gorelenkov, W. W. Heidbrink, A. Jaun, S. V. Konovalov, et al., Nucl. Fusion **47**, S264 (2007).
[2] W. W. Heidbrink, Phys. Plasmas **15**, 055501 (2008).
[3] S. Sharapov, B. Alper, H. Berk, D. Borba, and B. Breizman et al., Nuclear Fusion **53**, 104022 (2013).
[4] N. Gorelenkov, S. Pinches, and K. Toi, Nuclear Fusion **54**, 125001 (2014).
[5] K. G. McClements and E. D. fredrickson, Plasma Phys. Control. Fusion **59**, 053001 (2017).
[6] W. W. Heidbrink, M. A. VanZeeland, M. E. Austin, E. M. Bass, K. Ghantous, N. N. Gorelenkov, B. A. Grierson, D. A. Spong, and B. J. Tobias, Nuclear Fusion **53**, 093006 (2013).
[7] H. V. Wong and H. L. Berk, Phys. Lett. A **251**, 126 (1999).
[8] E. D. Fredrickson, R. V. Budny, D. S. Darrow, G. Y. Fu, J. Hosea, C. K. Phillips, and J. R. Wilson, Phys. Plasmas **7**, 4121 (2000).
[9] J. E. Menard, S. Gerhardt, M. Bell, J. Bialek, A. Brooks, J. Canik, J. Chrzanowski, M. Denault, L. Dudek, D. A. Gates, et al., Nucl. Fusion **52**, 083015 (2012).
[10] R. J. Hawryluk, in Physics of Plasmas Close to Thermonuclear Conditions (CEC, Brussels, 1980).
[11] For more details on the TRANSP code, please refer to the TRANSP webpage at http://w3.pppl.gov/~pshare/help/transp.htm.
[12] R. J. Goldston, D. C. McCune, H. H. Towner, S. L. Davis, R. J. Hawryluk, and G. L. Schmidt, J. Comput. Phys. **43**, 61 (1981).
[13] A. Pankin, D. McCune, R. Andre, G. Bateman, and A. Kritz, Computer Physics Communication **159**, 157 (2004).
[14] M. Podestà, M. Gorelenkova, and R. B. White, Plasma Phys. Control. Fusion **56**, 055003 (2014).
[15] M. Podestà, M. Gorelenkova, N. N. Gorelenkov, and R. B. White, Plasma Phys. Control. Fusion (submitted 2017).
[16] R. B. White and M. S. Chance, Phys. Fluids **27**, 2455 (1984).
[17] R. B. White, The theory of toroidally confined plasmas (Imperial College Press, London, UK, 2006), 2nd ed.
[18] S. D. Pinches, I. T. Chapman, P. W. Lauber, H. J. C. Oliver, S. E. Sharapov, K. Shinohara, and K. Tani, Phys. Plasmas **22**, 021807 (2015).

PPPL PRINCETON PLASMA PHYSICS LABORATORY

Princeton Plasma Physics Laboratory
Office of Reports and Publications

Managed by
Princeton University

under contract with the
U.S. Department of Energy
(DE-AC02-09CH11466)

P.O. Box 451, Princeton, NJ 08543
Phone: 609-243-2245
Fax: 609-243-2751

E-mail: publications@pppl.gov

Website: http://www.pppl.gov